Contents lists available at ScienceDirect

Chemical Engineering Research and Design

journal homepage: www.elsevier.com/locate/cherd

Impregnation of multiwall carbon nanotubes in alginate beads dramatically enhances their adsorptive ability to aqueous methylene blue

Bing Wang[a,b,c], *Bin Gao*[b,*], *Andrew R. Zimmerman*[d], *Xinqing Lee*[a,c]

[a] *State Key Laboratory of Environmental Geochemistry, Institute of Geochemistry, Chinese Academy of Sciences, Guiyang 550081, China*

[b] *Department of Agricultural and Biological Engineering, University of Florida, Gainesville, FL 32611, USA*

[c] *Puding Karst Ecosystem Research Station, State Key Laboratory of Environmental Geochemistry, Institute of Geochemistry, Chinese Academy of Sciences, Puding, 562100, China*

[d] *Department of Geological Sciences, University of Florida, Gainesville, FL 32611, USA*

ARTICLE INFO

Article history:
Received 9 November 2017
Received in revised form 15 March 2018
Accepted 16 March 2018
Available online 26 March 2018

Keywords:
Nanocomposites
Carbon nanotubes
Sorbents
Contaminant removal
Adsorption

ABSTRACT

In this work, novel environmentally benign nanocomposites, carboxyl functionalized multiwall carbon nanotubes (MWCNT-COOH) impregnated into calcium-alginate (CA) beads (CA-MWCNT-COOH), were tested for their abilities to remove a common dye contaminant, methylene blue (MB), from aqueous solution. Kinetic studies showed that the adsorption process of CA-MWCNT-COOH had similar speed to that of CA beads but was slower than that of undispersed MWCNT-COOH. With a Langmuir maximum MB adsorption capacity of 1189 mg g^{-1}, the CA-MWCNT-COOH performed best, outperforming both CA beads alone (1144.7 mg g^{-1}) and the undispersed MWCNT-COOH (33.4 mg g^{-1}). Furthermore, the impregnation also dramatically enhanced the adsorption of MB onto other types of MWCNTs, indicating CA beads are an excellent supporting material to disperse and stabilize carbon nanotubes for their optimal application as a high-capacity adsorbent.

1. Introduction

With the rapid development of the textile, printing and dyeing industry, dye wastewater emissions are increasing. The total dye consumption in the textile industry worldwide is more than 10,000 t/year and approximately 100 t/year of dyes is discharged into aquatic systems (Yagub et al., 2014). Dyes are responsible for water-borne diseases exhibiting symptoms such as hemorrhage, nausea, dermatitis, ulceration of skin and mucous membranes, kidney damage, and a loss of bone marrow leading to anemia (Tunç et al., 2013). Therefore, technologies are needed for the removal of dye from wastewater streams (Crini, 2006; Yagub et al., 2014). The traditional biological processing method is low in cost, but the degradation process is slow, and the treatment equipment requires a large land area. Alternative processing techniques adopted to treat dye wastewater include precipitation, flotation, ion exchange, solvent extraction, cementation onto iron, membrane filtration, chemical oxidation, coagulation, flocculation and electrochemical treatment (Sadri Moghaddam et al., 2010). For many of these technologies, such as electrochemical treatment, the equipment is simple and can be automated, but the treatment cost is high. Therefore, development of new low-cost and effective technologies for treating dyeing wastewater has become a research priority for governments and environmental engineers globally.

At present, the adsorption method is straightforward and has been widely used in the treatment of pollutants in water and air (Gupta et al., 2012b; Rafatullah et al., 2010). But improving adsorption efficiency is a great challenge. Various adsorbents and methods such as activated carbon (Ayranci and Duman, 2009), sepiolite (Duman et al., 2015b), vermiculite (Duman et al., 2015a), carbon nanotube (Duman et al., 2016a, 2016b) and photo-catalytic degradation (Gupta et al., 2012a, 2011b) were used to remove dyes from aqueous solution. In addition, activated carbon is the most widely used adsorbent to remove pollutants from water

* *Corresponding author.*
E-mail address: bg55@ufl.edu (B. Gao).
https://doi.org/10.1016/j.cherd.2018.03.026

(Ayranci and Duman, 2009, 2010; Duman and Ayranci, 2006, 2010a, 2010b). On the other hand, the application of activated carbon for a large-scale wastewater treatment is limited because of its high cost (Duman et al., 2015a). Therefore, a lot of research has been continued for inexpensive alternative adsorbents having reasonable adsorption efficiencies (Duman et al., 2015b). Nanomaterials show great potential for environmental remediation as they are excellent sorbents due to their large specific surface areas and high reactivity (Khin et al., 2012; Qu et al., 2013; Zhang and Gao, 2013). Carbon nanotubes (CNTs) are a new type of sorbent with the advantages of large adsorption capacity, fast adsorption rate and are effective on a wide range of sorptive (Gupta et al., 2011a, 2013; Inyang et al., 2014; Kuo et al., 2008; Saleh and Gupta, 2012; Wu, 2007). There are many kinds of CNTs being proposed as potential adsorbents for the treatment of dyeing wastewater, each having different characteristics. CNTs are usually between several hundred nanometers and tens of micrometers in length. However, due to the strong van der Waals attractive intermolecular forces, CNTs often exist in an entangled and aggregated states, lowering their effective specific surface area. In order to preserve the excellent adsorption performance of carbon nanotubes, a dispersive agent is required (Xie et al., 2005). Controversially, it is difficult to separate the well-dispersed CNTs completely from the water during the conventional water treatment process. A fixation or impregnation method is thus required to avoid nano-pollution caused by CNTs, which may affect the health of the environment and the human body (Aschberger et al., 2010; Lam et al., 2006).

Preparation of CNT nanocomposite materials can overcome the problems associated with the small size of CNTs, making them more useful to be used as an adsorbent in the environmental field (Jung et al., 2015; Saber-Samandari et al., 2017). Alginate is a natural polysaccharide product extracted from cold water brown seaweed. It has good sorptive ability due to its many organic functional groups (e.g. carboxylic and phenolic) and is environmentally benign. Because of these advantages, calcium alginate (CA) has been often used as the supporting material to impregnate a variety of engineered nanomaterials including CNTs to improve their dispersion and stability for environmental applications (Jung et al., 2015; Li et al., 2013; Qu et al., 2013).

There are more than 100,000 dyes that are commercially available, but our current research focuses on the removal of a common dye, methylene blue (MB), which is regarded as a very dangerous environment pollutant with negative human health effects even in small quantities (Nigam et al., 2000; Rafatullah et al., 2010). Because of its known strong adsorption onto solids, MB often serves as a model compound for studies of organic contaminant (e.g., organic dyes) removal from aqueous solutions by various adsorbents (Ding et al., 2016; Gimbert et al., 2008; Houas et al., 2001; Lyu et al., 2018; Zhang and Gao, 2013). The objectives of this study are as follows: (1) synthesis different types of CA-based multiwall CNT (MWCNT) nanocomposites; (2) investigate the adsorption behaviors of MB onto the nanocomposites; and (3) determine the effect of CA impregnation on the MB adsorption on different types of MWCNTs.

2. Experimental methods

2.1. Chemicals and reagents

Four different multiwall carbon nanotubes (MWCNTs) were purchased from Sinonano (Nanjing, China): (1) carboxylated (MWCNT-COOH), (2) hydroxylated (MWCNT-OH), (3) elemental sulfur functionalized (S-MWNT-1020) and (4) pristine (MWCNT). Sodium alginate from *Macrosytica pyrifera* (MP Biomedicals, Inc. Co., USA), calcium chloride ($CaCl_2$) and methylene blue (Acros Organics) were all purchased from Fisher Scientific. Stock solutions of MB (1000 mg L^{-1}) were prepared in deionized (DI) water which were further diluted to achieve desired concentrations. All the chemicals and reagents used in this study were of reagent grade and used without any further purification.

2.2. Preparation of the sorbents

To make beads of CA-MWCNT composites, sodium alginate was mixed with MWCNT and placed into a $CaCl_2$ solution, followed by sodium removal and dried. First, the MWCNTs were dispersed in DI water (1% w/v) using an ultrasonic cleaner (Model B3510-MT Branson Ultrasonics Co., USA) which had a nominal frequency of 40 kHz, for 2 h at 25 °C. The MWCNTs dispersion was thoroughly mixed with a suspension of sodium alginate (1% w/v) at the mass ratio of 0.25 (MWCNTs/alginate). Then, 100 mL of this colloidal solution was added dropwise into 500 mL of 0.1 M $CaCl_2$ solution while stirring. The alginate beads that formed were left overnight to stabilize. The beads were washed several times with deionized water to remove sodium, residual MWCNT particles, and non-cross-linked calcium ions. The beads were then dried in an oven at 50 °C for 24 h and used as the adsorbent in the adsorption experiment. To serve as controls, MWCNTs, as purchased, were used and CA beads were made by the above process but without the addition of MWCNT.

2.3. Characterizations of sorbents

The adsorbents were characterized using scanning electron microscope (SEM), elemental and surface analysis. The SEM was carried out to illustrate the surface morphology of the composites after drying. The samples were imaged with a beam energy of 20 kV on a JSM-6460LV SEM. The specific surface area and pore size distributions of the sorbents were measured by N_2 sorptometry on a Quantachrome Autosorb I, at 77 K. Samples were de-gassed under vacuum at least 24 h at 180 °C prior to analysis. The specific surface area was calculated according to BET theory using adsorption data in the 0.01–0.3 relative pressure range. Pore volumes were calculated using Barrett–Joyner–Halenda (BJH) theory using desorption leg data.

2.4. MB adsorption

Adsorption capacity and kinetics of MB on the sorbents (i.e., CA beads, MWCNTs, and nanocomposites) were all examined by mixing the sorbent with 40 mL of MB solutions in 50 mL centrifuge tubes (Fisher Scientific) at room temperature (22 ± 0.5 °C). The tubes were shaken on a New Brunswick table shaker at 60 rpm until sampling. To determine the adsorption kinetics, at each sampling time (0.083, 0.5, 1, 2, 4, 8, 16 and 24 h), the overlying suspensions were removed using a Pasteur pipette. Different MB initial concentrations were used to determine the adsorption isotherms and the sampling time was 24 h. For MWCNTs, samples were filtered using a 0.22 μm syringe filter (PVDF syringe filter; Whatman). Concentrations of MB in the solution were measured using a GENESYS 10S UV–vis spectrophotometer at 665 nm (Thermo Fisher Scientific). Regeneration of the CA-MWCNT-COOH beads was also tested. The CA-MWCNT-COOH beads were first loaded with MB of initial concentration of 50 mg L^{-1} (shaken for 24 h). After filtration, CA-MWCNT-COOH beads were added into 40 mL DI water and shaken for 24 h to desorb the MB. Four regeneration cycles were performed.

All the adsorption experiments were conducted in triplicate, and the average experimental data and standard deviation were reported. For comparison, a control experiment was carried out using the same procedure without adsorbents.

Table 1 – Basic characteristics of the four MWCNTs used in this study.

CNTs	Diameter (nm)	Length (μm)	Ash (wt %)	Specific surface area ($m^2\ g^{-1}$)
MWCNT	20–40	1–15	<2	227.3
MWCNT-COOH	>50	10–20	<1.5	86.6
MWCNT-OH	<2	5–15	<2	435.7
S-MWNT-1020	10–20	1–2	<2	127.4

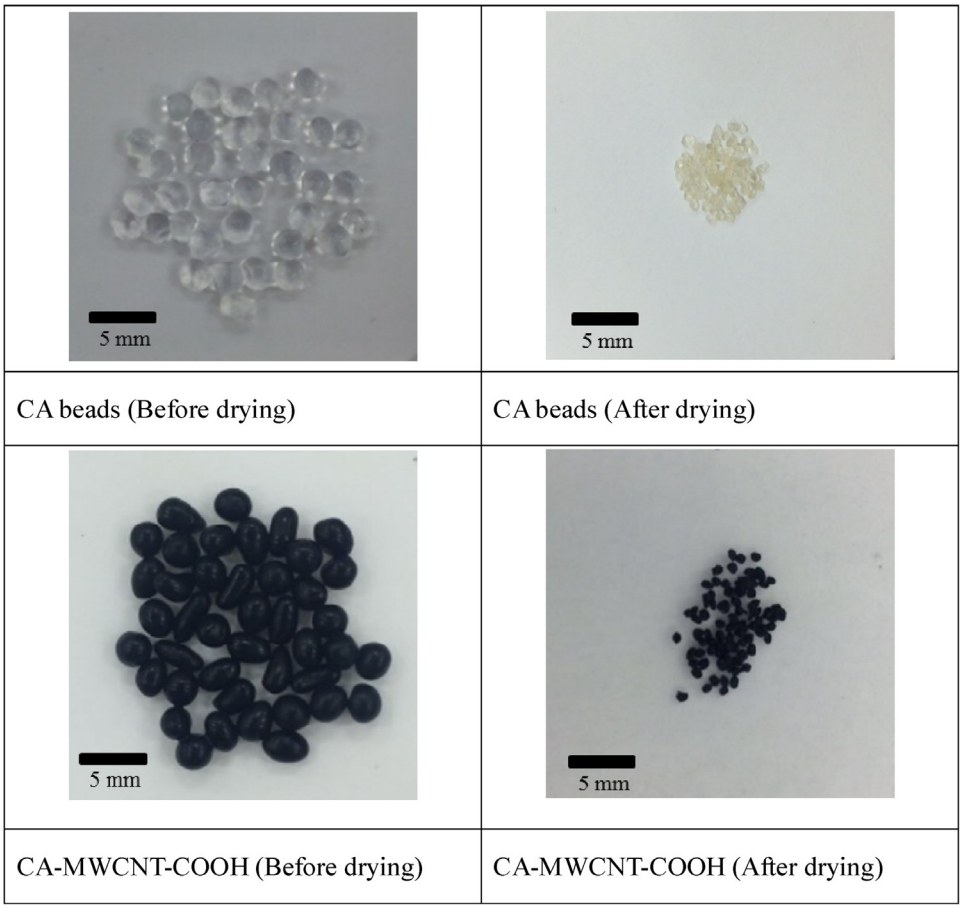

Fig. 1 – Photographs of alginate beads (CA) and alginate-carbon nanotube nanocomposites (CA-MWCNT-COOH) before and after drying.

Various models were used to simulate the adsorption kinetics and isotherms.

3. Results and discussion

3.1. *Characterization of sorbents*

The characteristics of four types of MWCNTs are listed in Table 1. All the CA-based sorbents displayed significant shrinkage after drying (Fig. 1). The diameters of non-dried and dried (CA and CA-MWCNTs) beads is 3.3 ± 0.1 mm and 0.76 ± 0.01 mm, respectively. SEM showed that the surface structures of the dried CA-MWCNT-OH and CA-MWCNT were relatively compact, while the internal structures of the dried CA-MWCNT-COOH and CA-S-MWNT-1020 were relatively more porous in texture, suggesting that the MWCNT-COOH and S-MWNT-1020 might have better ability to create pore space within the nanocomposites (Fig. 2).

3.2. *Adsorption kinetics*

The adsorption of MB (50 mg L^{-1} initial concentration) on MWCNT-COOH nanoparticles and dried CA and CA-MWCNT-COOH beads was studied as a function of contact time. The uptake process of MB for MWCNT-COOH was found to be fast with 92.8% of the adsorption completed in about 5 min (Fig. 3), suggesting the relatively fast external mass transfer was the rate-determining step. However, the adsorption of MB for both CA and CA-MWCNT-COOH exhibited a slower uptake, removing 75.5% of the MB within 8 h, and 82.5% within 16 h. This was due to the adsorption kinetics of MB on the nanocomposites were mainly controlled by the diffusive transport of the MB compounds within the pore network of the nanocomposites. There was no significant change in the amount of MB adsorption after about 24 h, the equilibration point. The adsorption capacity of CA-MWCNT-COOH for MB was 100.7 mg g^{-1}, which corresponded to 75.5% removal efficiency during the initial 8 h contact time. The equilibrium time found for CA-MWCNT-COOH in this study is longer than has been observed by others (Bulut and Aydın, 2006; Doğan et al., 2004), probably because of the differences in pore tortuosity of the nanocomposites.

Modeling the adsorption kinetic data helps to understand the potential rate-controlling steps and mechanisms in the adsorption process (Li et al., 2005). Pseudo-first-order,

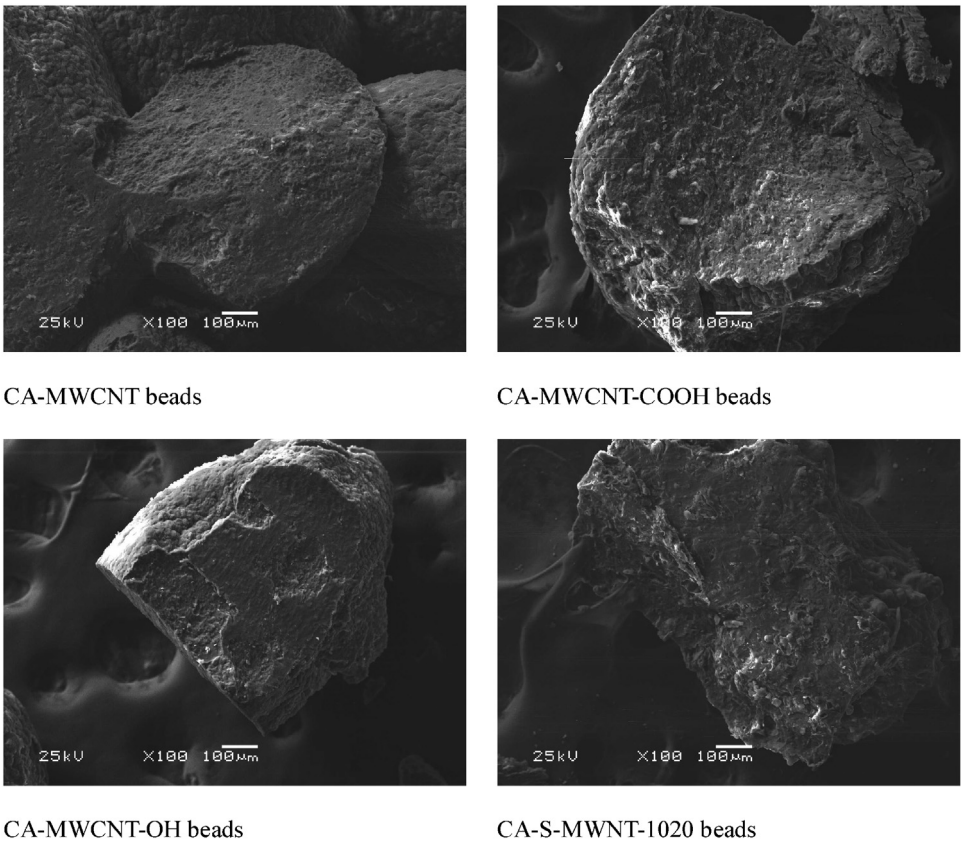

Fig. 2 – Scanning electron microscope (SEM) images of alginate-carbon nanotube nanocomposites (dried), cut to reveal their surface morphology. Samples were imaged with a beam energy of 25 kV on a JSM-6460LV SEM. See text for abbreviations.

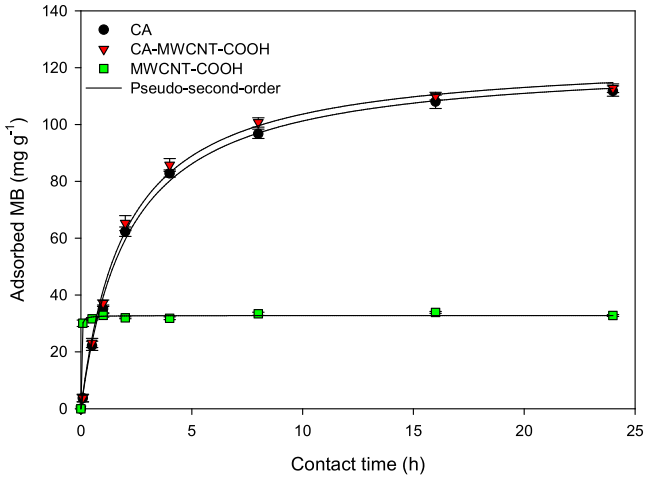

Fig. 3 – Adsorption kinetics of MB onto CA, MWCNT-COOH, and CA-MWCNT-COOH at initial MB concentration of 50 mg L^{-1}. The solid line is a pseudo-second-order kinetic model (discussed in the text). Error bars represent standard error of triplicate samples (n = 3). MWCNT-COOH dose 5 mg/40 mL, CA and CA-MWCNT-COOH dose 15 mg/40 mL.

pseudo-second-order, Elovich and Ritchie models were used to simulate the adsorption kinetic data.

$$q_t = q_e(1 - e^{-k_1 t}), \quad \text{Pseudo-first-order} \tag{1}$$

$$q_t = \frac{k_2 q_e^2 t}{1 + k_2 q_e t}, \quad \text{Pseudo-second-order} \tag{2}$$

$$q_t = \frac{1}{\beta}\ln(\alpha\beta t + 1), \quad \text{Elovich} \tag{3}$$

$$q_t = q_e - \left(q_e^{1-n}\frac{k_n}{1-n}t\right)^{\frac{1}{1-n}}, \quad \text{Ritchie} \tag{4}$$

where q_t (mg g^{-1}) and q_e (mg g^{-1}) are the amounts of MB sorbed at time t and at equilibrium, respectively; k_1 (h^{-1}), k_2 (g mg^{-1} h^{-1}), and k_n (g^{n-1} mg^{1-n} h^{-1}) are the pseudo-first-order, pseudo-second-order, and Ritchie n_{th}-order adsorption rate constants, α (mg g^{-1} h^{-1}) is the initial adsorption rate; and β (g mg^{-1}) is the desorption constant.

Among all the tested models, the pseudo-second-order models described the MB adsorption kinetics better than the other models (Table 2). This suggests that the adsorption of MB follows pseudo-second-order kinetics and there might be multiple sites or processes involved. In the initial stage, the higher driving force allowed external mass transfer resistances to be overcome, and active sites with a higher affinity were occupied. Once the high-affinity binding sites are occupied, residual binding sites with a lower affinity become occupied, leading to the slow attainment of equilibrium.

3.3. *Sorbent dosage*

Given the 24 h was found to be sufficient for adsorption to reach equilibrium all further experiments were carried out over this duration. The CA-MWCNT-COOH dosage was varied from 2.5 mg to 25 mg with initial MB concentration 50 mg L^{-1}. On a sorbent weight-normalized basis, the adsorbed MB amount decreased with increasing sorbents dosage when the dosage was between 50 and 250 mg L^{-1}, while the removal rate (%) increased (Fig. 4). When the amount of sorbents dosage was increased above 250 mg L^{-1}, adsorption loading reached a plateau. Similarly, MB removal rate efficiency increased read-

Table 2 – Summary of the best-fit parameters of various kinetic models for MB adsorption onto the studied sorbents.

Adsorbent	Model	Parameter 1	Parameter 2	R^2
CA	Pseudo-first-order	$k_1 = 0.399$	$q_e = 107.2$	0.995
	Pseudo-second-order	$k_2 = 0.00383$	$q_e = 122.7$	0.998
	Elovich	$\alpha = 102.2$	$\beta = 0.0381$	0.981
	Ritchie	$k_n = 0.0102$	$q_e = 114.3$	0.998
MWCNT-COOH	Pseudo-first-order	$k_1 = 30.6$	$q_e = 32.6$	0.995
	Pseudo-second-order	$k_2 = 3.84$	$q_e = 32.8$	0.996
	Elovich	$\alpha = 896$	$\beta = 0.201$	0.440
	Ritchie	$k_n = 1.69$	$q_e = 32.6$	0.996
CA-MWCNT-COOH	Pseudo-first-order	$k_1 = 0.421$	$q_e = 109.1$	0.996
	Pseudo-second-order	$k_2 = 0.00405$	$q_e = 124.3$	0.997
	Elovich	$\alpha = 113.8$	$\beta = 0.0383$	0.977
	Ritchie	$k_n = 0.0114$	$q_e = 113.8$	0.998

Note: Initial MB concentration 50 mg L^{-1}, MWCNT-COOH dose 5 mg/40 mL, CA and CA-MWCNT-COOH dose 15 mg/40 mL. Model equations and parameters are described in the text.

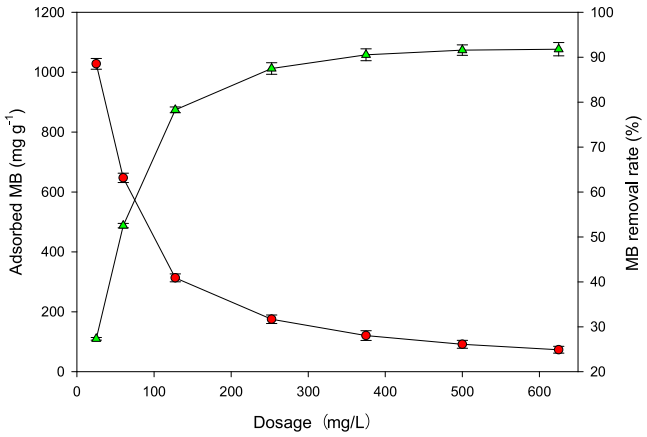

Fig. 4 – Effect of CA-MWCNT-COOH dosage on MB adsorption capacity (circles) and removal rate (triangles) at initial MB concentration 50 mg L^{-1} (24 h contact time). Error bars represent standard error of triplicate samples (n = 3).

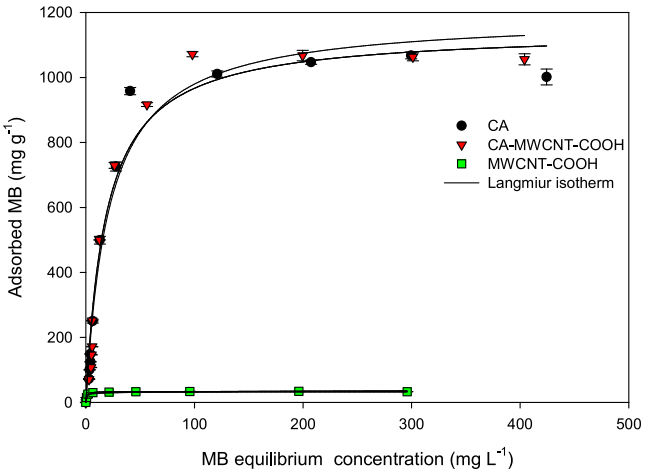

Fig. 5 – Adsorption isotherms of MB onto CA, MWCNT-COOH, and CA-MWCNT-COOH. Data modeled uses Langmuir model (solid lines). Error bars represent standard error of triplicate samples (n = 3). Symbols may cover error bars. Contact time 24 h, MWCNT-COOH dose 5 mg/40 mL, CA and CA-MWCNT-COOH dose 15 mg/40 mL.

ily with increasing sorbent dosage until about 250 mg L^{-1}, after which removal rate increased to a maximum of 91%. This can be interpreted as an indicating a surface site adsorption mechanism in which binding sites become nearly saturated at a specific loading (250 mg L^{-1} dosage). A similar mechanism was also shown in other studies (Jin et al., 2008). Hence, optimum CA-MWCNT-COOH dosage for removal of MB was found to be about 250 mg L^{-1} of CA-MWCNT-COOH for initial MB concentration 50 mg L^{-1}.

3.4. *Adsorption isotherms*

Equilibrium MB adsorption isotherms of CA, MWCNT-COOH, and CA-MWCNT-COOH were generated using a dosage of 15 mg dry weight per 40 mL solution and a 24 h contact time (Fig. 5). Adsorption of MB increased rapidly up to an equilibrium MB concentration of about 100 mg L^{-1} than leveled off rapidly. Equilibrium adsorption isotherm modeling was used to better understand the mechanism of adsorption and to identify the maximum adsorption capacity of each material. Several mathematical models have been used for describing equilibrium studies for the removal of pollutants by adsorption data were fitted to both Freundlich and Langmuir isotherm models using the following equations:

$$\text{Langmuir isotherm}: q_e = Q_m k_L \cdot C_e/(1 + k_L C_e) \quad (5)$$

$$\text{Freundlich isotherm}: q_e = k_f C_e^{1/n} \quad (6)$$

where q_e (mg g^{-1}) is the adsorption capacity; Q_m (mg g^{-1}) is the maximum adsorption capacity; C_e (mg L^{-1}) is the equilibrium concentration after the adsorption or desorption; k_L (L mg^{-1}) is a Langmuir constant; k_f ($mg^{1-1/n}$ $L^{1/n}$ g^{-1}) is the Freundlich adsorption constant; 1/n (dimensionless) is the adsorption affinity.

The Langmuir model presumes that adsorption on a homogenous surface is a monolayer process without any interactions among adsorbed ions. The Freundlich model is based on the assumption that the adsorption of sorbent ions occurs on a heterogeneous surface and may involve multiple mechanisms. Although the Langmuir and the Freundlich models cannot provide conclusive proofs of the adsorption mechanisms, they are commonly used in the literature as a powerful tool to interpret isotherms to reveal adsorption mechanisms (Liu et al., 2012; Wang et al., 2018). For all three sorbents, the Langmuir equation simulated the data better than the Freundlich equation (i.e. higher R^2 in Table 3),

Table 3 – Summary of the best-fit isotherm model parameters for MB adsorption onto the studied sorbents.

Adsorbent	Langmuir adsorption model			Freundlich adsorption model		
	Q_m (mg MB g^{-1})	k_L (L mg^{-1})	R^2	k_f ($mg^{1-1/n}$ $L^{1/n}$ g^{-1})	$1/n$	R^2
CA	1144.7	0.0544	0.9712	195.4	0.304	0.8308
MWCNT-COOH	33.4	1.63	0.9978	22.6	0.0816	0.9236
CA-MWCNT-COOH	1189.0	0.0468	0.9752	186.5	0.318	0.8452

Note: Initial methylene blue concentration 30–800 mg L^{-1}, MWCNT-COOH dose 5 mg/40 mL, CA and CA-MWCNT-COOH dose 15 mg/40 mL. Model equations and parameters are described in the text.

Table 4 – Previously reported adsorption capacities of MB onto various sorbents.

Sorbent	Q_m (mg g^{-1})	pH	Temperature (°C)	Ref.
Activated carbon	454.2	7.0	30	Hameed et al. (2007)
Carbon nanotubes	46.2	7.0	25	Yao et al. (2010)
M-MWCNTs	48.06	–	25	Ai et al. (2011)
Alg-HNT hybrid beads	222	–	25	Liu et al. (2012)
Ca-alginate/AC beads	892	7.5	20	Hassan et al. (2014)
Calcium alginate beads	800	7.5	20	Hassan et al. (2014)
GO/Ca-alginate composites	181.81	5.4	25	Li et al. (2013)
Montmorillonite clay	289.12	–	35	Almeida et al. (2009)
MWCNTs	109.31	–	27	Zohre et al. (2010)
Ca-alginate bentonite AC beads	756.97	–	30	Benhouria et al. (2015)
CA-MWCNT-COOH	1189	–	22	This study

Note: M-MWCNT = magnetic magnetite (Fe_3O_4)-loaded multiwall carbon nanotubes, Alg-HNT hybrid beads = alginate-halloysite nanotube hybrid beads, GO/Ca-alginate composites = graphene oxide/Ca-alginate composites.

suggesting that the adsorption process might be monomolecular. The Freundlich constant, $1/n$, is the concentration index that represents the degree of linearity of the isotherm. In this study, the $1/n$ constants of the three adsorbens were less than 1, suggesting that these materials interacted with MB might be a favorable adsorption process (Li et al., 2013). The calculated adsorption capacities of CA, MWCNT-COOH, and CA-MWCNT-COOH were found to be 1144.7, 33.4, and 1189.0 mg g^{-1}, respectively. The MB adsorption capacity of CA-MWCNT-COOH is higher than that of CA and MWCNT-COOH. This may be because, after impregnating into CA, the MWCNT-COOH became more stable and was homogeneously distributed in the beads with larger specific surface area and thus more adsorption sites for MB. Compared with many other adsorbents, including other CNT-alginate composites, the CA-MWCNT-COOH in this work showed higher MB adsorption capacity (Table 4).

Although the undispersed MWCNT-COOH showed much lower MB adsorption capacity than CA, the maximum capacity of their composite (CA-MWCNT-COOH) increased by 44.3 and 1155.6 mg g^{-1} compared with CA and MWCNT-COOH, respectively. This result indicated that MB adsorption capacity of the impregnated MWCNT-COOH became higher than that of CA, confirming impregnation dramatically enhanced its adsorption capacity. The impregnation enhanced the dispersion of the MWCNT-COOH within the CA bead to adsorb MB through following potential mechanisms: (1) increasing the carboxyl groups (—COOH) to adsorb the cationic MB compounds through electrostatic attraction; and (2) exposing the basal-plane of the MWCNT-COOH to adsorb the MB through π–π interaction (Jeon et al., 2008; Rocher et al., 2008; Zhuang et al., 2016). In CA-MWCNT-COOH, there are 80% of CA and 20% of MWCNT-COOH. It is reasonable to assume that the impregnation had little effect on the sorptive property of the CA and thus the enhanced MB adsorption was mainly from the contribution of the impregnated MWCNT-COOH. Based mass balance calculation, the maximum MB adsorption capacity of the impregnated MWCNT-COOH in the nanocomposite should be 1366.2 mg g^{-1}, which is more than 40 times of that of the undispersed MWCNT-COOH (i.e., 33.4 mg g^{-1}). The adsorption capacity of MB on CA-MWCNT-COOH nanocomposite in this work is higher than that of CA/AC (calcium alginate/activated carbon) beads and CA beads that have been reported previously in other studies (Hassan et al., 2014).

3.5. *Regeneration*

To evaluate the regeneration of CA-MWCNT-COOH nanocomposite, desorption experiments were conducted repeatly using 40 mL DI water (each time) to desorb the extract MB from post-adsorption samples (initial concentration of 50 mg L^{-1}). Most of the adsorbed MB was desorbed by water after four cycles. In the first three cycles, about 90% of the adsorbed MB was extracted, and less than 10% was extracted for the fourth cycle (Fig. 6). This result indicates that the nanocomposite can be used as a regenerative absorbent. Meanwhile, there was no obvious change in the shape of the CA-MWCNT-COOH nanocomposite after the extraction. This suggests that the regeneration of adsorbents is feasible.

3.6. *Other MWCNTs*

Finally, MB adsorption capacities of all the undispersed and CA-impregnated MWCNTs were compared at sorbate concentrations near their maximum adsorption capacity (initial MB concentration of 500 mg L^{-1}) (Fig. 7). While two of undispersed MWCNTs had greater MB adsorption capacities than undispersed MWCNT-COOH (52.44 mg g^{-1} and 71.84 mg g^{-1} for MWNT-1020 and MWCNT, respectively), they did not perform as well as MWCNT-COOH when impregnated within CA beads. CA-impregnated MWNT-OH, MWNT-1020 and MWCNT sorbed MB significantly less than MWCNT-COOH by 12.7%, 3.25%, and

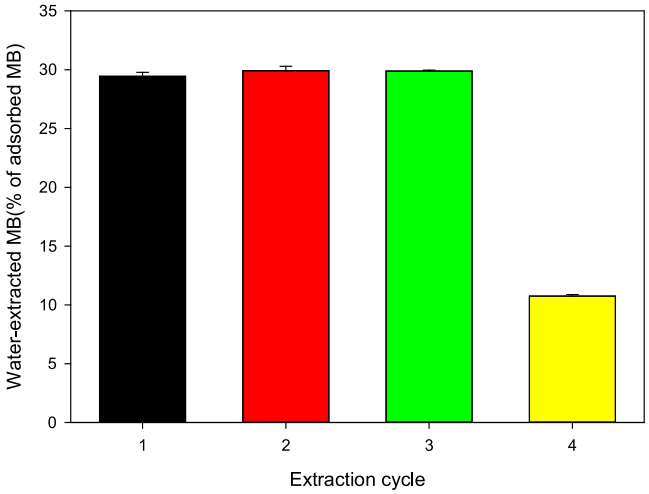

Fig. 6 – Water-extracted MB from different extraction cycles. Solution volume 40 mL, temperature 298 K, and contact time 24 h.

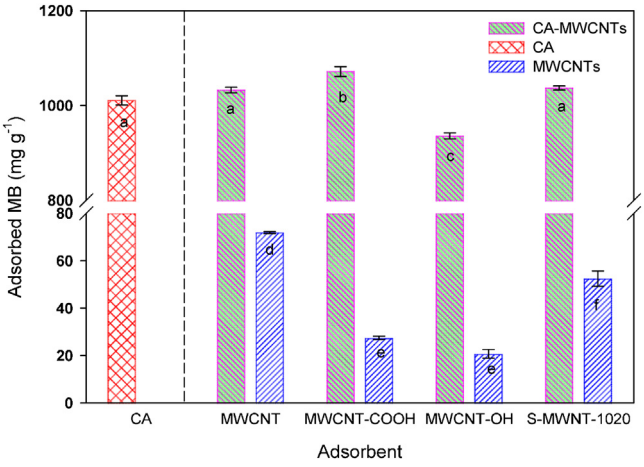

Fig. 7 – Adsorption of methylene blue (MB) at near maximum adsorption capacity (initial MB concentration of 500 mg L^{-1}, contact time 24 h) by calcium alginate beads (CA) and undispersed and CA-impregnated MWCNTs. Error bars represent standard error of triplicate samples (n = 3). Different letters denote samples with significant differences in sorbed MB (mg g^{-1}) at $p < 0.01$. MWCNT dose 5 mg/40 mL, CA and CA-MWCNT dose 15 mg/40 mL.

3.66%, respectively. This result suggested that, while alginate beads severed as a good supporting material for all the tested MWCNTs, it might disperse the carboxyl-functionalized one better than the others.

4. Conclusions

Kinetic studies showed that MB adsorption by CA-MWCNT-COOH reached equilibrium within 8 h, which is similar to the adsorption kinetics of the CA but much slower than that of the undispersed MWCNT-COOH. This confirmed the impregnation of MWCNT-COOH into the pore networks of CA beads. Isotherm studies showed that MB adsorption by the sorbents followed the order of CA-MWCNT-COOH > CA » MWCNT-COOH, indicating the impregnation dramatically enhanced the sorptive ability of the MWCNT. The Langmuir maximum MB adsorption capacity of the impregnated MWCNT-COOH in the nanocomposite (1366.2 mg g^{-1}) was more than 40 times of that of the undispersed MWCNT-COOH (33.4 mg g^{-1}). The impregnation also dramatically enhanced the adsorption of MB onto other types of MWCNTs and the CA-MWCNT-COOH showed the best performance. Because only immobilized CNTs are likely stabilized to the degree needed for water or soil treatment, CA bead as a supporting material thus provides an excellent way for these applications. Further studies are needed to explore the removal of other contaminants by CA-CNT nanocomposites and to measure their long-term stability.

Acknowledgments

This work was financially supported by the National Key Research and Development Program of China (2016YFC0502602), the National Natural Science Foundation of China (U1612441), the International Scientific and Technological Cooperation Project of Guizhou Province (G[2012]7050), the "Dawn of West China" Talent Training Program of the Chinese Academy of Sciences ([2012]179), and the Opening Fund of State Key Laboratory of Environmental Geochemistry (2018907).

References

Ai, L., et al., 2011. Removal of methylene blue from aqueous solution with magnetite loaded multi-wall carbon nanotube: kinetic, isotherm and mechanism analysis. J. Hazard. Mater. 198, 282–290.

Almeida, C., Debacher, N., Downs, A., Cottet, L., Mello, C., 2009. Removal of methylene blue from colored effluents by adsorption on montmorillonite clay. J. Colloid Interface Sci. 332 (1), 46–53.

Aschberger, K., et al., 2010. Review of carbon nanotubes toxicity and exposure—appraisal of human health risk assessment based on open literature. Crit. Rev. Toxicol. 40 (9), 759–790.

Ayranci, E., Duman, O., 2009. In-situ UV-visible spectroscopic study on the adsorption of some dyes onto activated carbon cloth. Sep. Sci. Technol. 44 (15), 3735–3752.

Ayranci, E., Duman, O., 2010. Structural effects on the interactions of benzene and naphthalene sulfonates with activated carbon cloth during adsorption from aqueous solutions. Chem. Eng. J. 156 (1), 70–76.

Benhouria, A., Islam, M.A., Zaghouane-Boudiaf, H., Boutahala, M., Hameed, B.H., 2015. Calcium alginate–bentonite–activated carbon composite beads as highly effective adsorbent for methylene blue. Chem. Eng. J. 270, 621–630.

Bulut, Y., Aydın, H., 2006. A kinetics and thermodynamics study of methylene blue adsorption on wheat shells. Desalination 194 (1–3), 259–267.

Crini, G., 2006. Non-conventional low-cost adsorbents for dye removal: a review. Bioresour. Technol. 97 (9), 1061–1085.

Ding, Z.H., et al., 2016. Sorption of lead and methylene blue onto hickory biochars from different pyrolysis temperatures: importance of physicochemical properties. J. Ind. Eng. Chem. 37, 261–267.

Doğan, M., Alkan, M., Türkyilmaz, A., Özdemir, Y., 2004. Kinetics and mechanism of removal of methylene blue by adsorption onto perlite. J. Hazard. Mater. 109 (1–3), 141–148.

Duman, O., Ayranci, E., 2006. Adsorption characteristics of benzaldehyde, sulphanilic acid, and *p*-phenolsulfonate from water, acid, or base solutions onto activated carbon cloth. Sep. Sci. Technol. 41 (16), 3673–3692.

Duman, O., Ayranci, E., 2010a. Adsorptive removal of cationic surfactants from aqueous solutions onto high-area activated carbon cloth monitored by in situ UV spectroscopy. J. Hazard. Mater. 174 (1), 359–367.

Duman, O., Ayranci, E., 2010b. Attachment of benzo-crown ethers onto activated carbon cloth to enhance the removal of chromium, cobalt and nickel ions from aqueous solutions by adsorption. J. Hazard. Mater. 176 (1), 231–238.

Duman, O., Tunç, S., Bozoğlan, B.K., Polat, T.G., 2016a. Removal of triphenylmethane and reactive azo dyes from aqueous solution by magnetic carbon nanotube-κ-carrageenan-Fe_3O_4 nanocomposite. J. Alloys Compd. 687, 370–383.

Duman, O., Tunç, S., Polat, T.G., 2015a. Determination of adsorptive properties of expanded vermiculite for the removal of CI Basic Red 9 from aqueous solution: kinetic, isotherm and thermodynamic studies. Appl. Clay Sci. 109, 22–32.

Duman, O., Tunç, S., Polat, T.G., Bozoğlan, B.K., 2016b. Synthesis of magnetic oxidized multiwalled carbon nanotube-κ-carrageenan-Fe_3O_4 nanocomposite adsorbent and its application in cationic Methylene Blue dye adsorption. Carbohydr. Polym. 147 (Supplement C), 8–79.

Duman, O., Tunc, S., Polat, T.G., 2015b. Adsorptive removal of triarylmethane dye (Basic Red 9) from aqueous solution by sepiolite as effective and low-cost adsorbent. Microporous Mesoporous Mater. 210, 176–184.

Gimbert, F., Morin-Crini, N., Renault, F., Badot, P.-M., Crini, G., 2008. Adsorption isotherm models for dye removal by cationized starch-based material in a single component system: error analysis. J. Hazard. Mater. 157 (1), 34–46.

Gupta, V.K., Agarwal, S., Saleh, T.A., 2011a. Synthesis and characterization of alumina-coated carbon nanotubes and their application for lead removal. J. Hazard. Mater. 185 (1), 17–23.

Gupta, V.K., et al., 2012a. Photo-catalytic degradation of toxic dye amaranth on TiO_2/UV in aqueous suspensions. Mater. Sci. Eng. C 32 (1), 12–17.

Gupta, V.K., Jain, R., Nayak, A., Agarwal, S., Shrivastava, M., 2011b. Removal of the hazardous dye—tartrazine by photodegradation on titanium dioxide surface. Mater. Sci. Eng. C 31 (5), 1062–1067.

Gupta, V.K., Kumar, R., Nayak, A., Saleh, T.A., Barakat, M.A., 2013. Adsorptive removal of dyes from aqueous solution onto carbon nanotubes: a review. Adv. Colloid Interface Sci. 193–194, 24–34.

Gupta, V.K., Mittal, A., Jhare, D., Mittal, J., 2012b. Batch and bulk removal of hazardous colouring agent Rose Bengal by adsorption techniques using bottom ash as adsorbent. RSC Adv. 2 (22), 8381–8389.

Hameed, B.H., Din, A.T.M., Ahmad, A.L., 2007. Adsorption of methylene blue onto bamboo-based activated carbon: kinetics and equilibrium studies. J. Hazard. Mater. 141 (3), 819–825.

Hassan, A., Abdel-Mohsen, A., Fouda, M.M., 2014. Comparative study of calcium alginate, activated carbon, and their composite beads on methylene blue adsorption. Carbohydr. Polym. 102, 192–198.

Houas, A., et al., 2001. Photocatalytic degradation pathway of methylene blue in water. Appl. Catal. B: Environ. 31 (2), 145–157.

Inyang, M., Gao, B., Zimmerman, A., Zhang, M., Chen, H., 2014. Synthesis, characterization, and dye sorption ability of carbon nanotube–biochar nanocomposites. Chem. Eng. J. 236, 39–46.

Jeon, Y.S., Lei, J., Kim, J.-H., 2008. Dye adsorption characteristics of alginate/polyaspartate hydrogels. J. Ind. Eng. Chem. 14 (6), 726–731.

Jin, X., Jiang, M.-q., Shan, X.-q., Pei, Z.-g., Chen, Z., 2008. Adsorption of methylene blue and orange II onto unmodified and surfactant-modified zeolite. J. Colloid Interface Sci. 328 (2), 243–247.

Jung, W., et al., 2015. Sorptive removal of heavy metals with nano-sized carbon immobilized alginate beads. J. Ind. Eng. Chem. 26, 364–369.

Khin, M.M., Nair, A.S., Babu, V.J., Murugan, R., Ramakrishna, S., 2012. A review on nanomaterials for environmental remediation. Energy Environ. Sci. 5 (8), 8075–8109.

Kuo, C.-Y., Wu, C.-H., Wu, J.-Y., 2008. Adsorption of direct dyes from aqueous solutions by carbon nanotubes: determination of equilibrium, kinetics and thermodynamics parameters. J. Colloid Interface Sci. 327 (2), 308–315.

Lam, C.-w., James, J.T., McCluskey, R., Arepalli, S., Hunter, R.L., 2006. A review of carbon nanotube toxicity and assessment of potential occupational and environmental health risks. Crit. Rev. Toxicol. 36 (3), 189–217.

Li, Y.-H., et al., 2005. Adsorption thermodynamic, kinetic and desorption studies of Pb^{2+} on carbon nanotubes. Water Res. 39 (4), 605–609.

Li, Y., et al., 2013. Methylene blue adsorption on graphene oxide/calcium alginate composites. Carbohydr. Polym. 95 (1), 501–507.

Liu, L., et al., 2012. The removal of dye from aqueous solution using alginate-halloysite nanotube beads. Chem. Eng. J. 187, 210–216.

Lyu, H., et al., 2018. Experimental and modeling investigations of ball-milled biochar for the removal of aqueous methylene blue. Chem. Eng. J. 335, 110–119.

Nigam, P., Armour, G., Banat, I.M., Singh, D., Marchant, R., 2000. Physical removal of textile dyes from effluents and solid-state fermentation of dye-adsorbed agricultural residues. Bioresour. Technol. 72 (3), 219–226.

Qu, X., Alvarez, P.J.J., Li, Q., 2013. Applications of nanotechnology in water and wastewater treatment. Water Res. 47 (12), 3931–3946.

Rafatullah, M., Sulaiman, O., Hashim, R., Ahmad, A., 2010. Adsorption of methylene blue on low-cost adsorbents: a review. J. Hazard. Mater. 177 (1–3), 70–80.

Rocher, V., Siaugue, J.-M., Cabuil, V., Bee, A., 2008. Removal of organic dyes by magnetic alginate beads. Water Res. 42 (4), 1290–1298.

Saber-Samandari, S., Saber-Samandari, S., Joneidi-Yekta, H., Mohseni, M., 2017. Adsorption of anionic and cationic dyes from aqueous solution using gelatin-based magnetic nanocomposite beads comprising carboxylic acid functionalized carbon nanotube. Chem. Eng. J. 308, 1133–1144.

Sadri Moghaddam, S., Alavi Moghaddam, M.R., Arami, M., 2010. Coagulation/flocculation process for dye removal using sludge from water treatment plant: optimization through response surface methodology. J. Hazard. Mater. 175 (1–3), 651–657.

Saleh, T.A., Gupta, V.K., 2012. Column with CNT/magnesium oxide composite for lead(II) removal from water. Environ. Sci. Pollut. Res. 19 (4), 1224–1228.

Tunç, S., Duman, O., Gürkan, T.l., 2013. Monitoring the decolorization of Acid Orange 8 and Acid Red 44 from aqueous solution using Fenton's reagents by online spectrophotometric method: effect of operation parameters and kinetic study. Ind. Eng. Chem. Res. 52 (4), 1414–1425.

Wang, B., Gao, B., Wan, Y., 2018. Comparative study of calcium alginate, ball-milled biochar, and their composites on aqueous methylene blue adsorption. Environ. Sci. Pollut. Res., http://dx.doi.org/10.1007/s11356-018-1497-1.

Wu, C.-H., 2007. Adsorption of reactive dye onto carbon nanotubes: equilibrium, kinetics and thermodynamics. J. Hazard. Mater. 144 (1–2), 93–100.

Xie, X.-L., Mai, Y.-W., Zhou, X.-P., 2005. Dispersion and alignment of carbon nanotubes in polymer matrix: a review. Mater. Sci. Eng. R: Rep. 49 (4), 89–112.

Yagub, M.T., Sen, T.K., Afroze, S., Ang, H.M., 2014. Dye and its removal from aqueous solution by adsorption: a review. Adv. Colloid Interface Sci. 209, 172–184.

Yao, Y., Xu, F., Chen, M., Xu, Z., Zhu, Z., 2010. Adsorption behavior of methylene blue on carbon nanotubes. Bioresour. Technol. 101 (9), 3040–3046.

Zhang, M., Gao, B., 2013. Removal of arsenic, methylene blue, and phosphate by biochar/AlOOH nanocomposite. Chem. Eng. J. 226, 286–292.

Zhuang, Y., Yu, F., Chen, J., Ma, J., 2016. Batch and column adsorption of methylene blue by graphene/alginate nanocomposite: comparison of single-network and double-network hydrogels. J. Environ. Chem. Eng. 4 (1), 147–156.

Zohre, S., Ataallah, S.G., Mehdi, A., 2010. Experimental study of methylene blue adsorption from aqueous solutions onto carbon nano tubes. Int. J. Water Resour. Environ. Eng. 2 (2), 016–028.